[CANCER RESEARCH 63, 2016–2019, May 1, 2003]

Advances in Brief

Preinvasive Pancreatic Neoplasia of Ductal Phenotype Induced by Acinar Cell Targeting of Mutant Kras in Transgenic Mice[1]

Paul J. Grippo,[2] Patrick S. Nowlin, Michael J. Demeure,[3] Daniel S. Longnecker, and Eric P. Sandgren[4]

Department of Pathobiological Sciences, School of Veterinary Medicine, University of Wisconsin-Madison, Madison, Wisconsin 53706 [P. J. G., P. S. N., E. P. S.]; Department of Surgery, Medical College of Wisconsin, Milwaukee, Wisconsin 53226 [P. J. G., M. J. D.]; and Department of Pathology, Dartmouth Medical School, Hanover, New Hampshire 03755 [D. S. L.]

Abstract

Activating mutation of the Kras oncogene is the most frequent and perhaps the earliest genetic alteration associated with pancreatic cancer. To examine the link between mutant Kras and exocrine pancreatic cancer, we generated transgenic mice carrying an elastase-mutant Kras transgene, which targets expression to pancreatic acinar cells. Most elastase-Kras founder mice displayed perinatal pancreatic acinar cell hyperplasia and dysplasia. However, adult mice in two surviving lineages displayed preinvasive pancreatic neoplastic lesions with ductal morphology, thereby providing a unique mouse model in which lesion histotype and initiating genetic alteration overlap with the human disease. Our findings suggest that Kras mutation is associated with development of early stage duct-like lesions in pancreas, but that additional alterations must accompany progression to malignancy.

Introduction

Pancreatic adenocarcinoma is diagnosed in ~1 in 10,000 people/year in the United States, and is the fifth leading cause of cancer death, with a 3% 5-year survival rate after diagnosis (1). Radiation and chemotherapy have proven ineffective as cures, and surgical resection of the tumor(s) and surrounding tissue provides a 5-year survival of only 20%. Poor survival after diagnosis can be attributed both to lack of early detection and the frequent metastasis of primary neoplasms into lymph nodes and organs surrounding the pancreas, including liver and stomach. To establish more effective treatment for pancreatic cancer, it is imperative to understand the molecular events leading to the onset and progression of this disease. Activating mutation of the *Kras* oncogene is the most frequent genetic alteration associated with pancreatic cancer, having been identified in up to 90% of all pancreatic adenocarcinomas (2, 3). Ras is a farnesylated, membrane-bound, monomeric G-protein that is active when bound to GTP. Ras proteins are involved in a variety of cell signaling pathways that are linked to mitogenic signaling and cellular differentiation. Kras can be activated by a point mutation at codons 12, 13, or 61 (2, 3). These mutations essentially "lock" ras into its active state (bound to GTP), causing constitutive activation of downstream signaling cascades. In human pancreatic adenocarcinoma, an amino acid substitution of either val or asp in place of gly of Kras codon 12 ($Kras^{V12G}$ or $Kras^{D12G}$) are identified most commonly. To explore the mechanistic relationship between expression of mutant *Kras* and exocrine pancreatic cancer, we generated transgenic mice carrying an Ela^5-$Kras^{D12G}$ transgene, which targets the Kras codon 12 aspartate mutant to pancreatic acinar cells. Most human pancreatic neoplasms have a ductal morphology (3), but transgene targeting strategies have not been developed that are specific for pancreatic ductal epithelium (4). However, several reports using both *in vitro* and *in vivo* experimental approaches suggest that injured or transformed acinar cells may assume a ductal phenotype (4–17). This information encouraged us to target mutant Kras using the well-characterized acinar cell-specific Ela enhancer/promoter.

Materials and Methods

Transgene Construction and Generation of Transgenic Mice. A genomic clone encoding human $Kras^{G12D}$, exons 1–4 in pMLD12 (provided by Dr. Manuel Perucho, La Jolla Cancer Research Center, La Jolla, CA) was subcloned in two fragments into a modified pSp72 (Promega, Madison, WI). The complete $Kras^{G12D}$ coding region was isolated from this plasmid and ligated into the pBluescript-based plasmid (Stratagene, La Jolla, CA) pBS-hsEla-human growth hormone, which contained: (*a*) the 200-bp Ela enhancer/promoter; (*b*) a unique *Bam*HI site; and (*c*) 650-bp of the human growth hormone gene containing the 3′ polyadenylation signal, all flanked by (*d*) hypersensitive site-containing loci (10 kb 5′ and 7 kb 3′) that are located 5′ and 3′ of the metallothionein gene locus (18). The transgene, designated Ela-$Kras^{G12D}$, was microinjected into the pronucleus of fertilized single-cell FVB strain (Taconic, Germantown, NY) eggs. To identify transgenic mice, DNA was extracted from a 2-mm tail biopsy. A 1 μl aliquot of supernatant was used in a PCR reaction mix containing the following primer pairs: 5′-GAGTGC-CGGCCTTGTTCTGTCTTTG-3′ (forward) and 5′-CTACGCCACAAGCTC-CAACTACCAC-3′ (reverse). The reaction mixture was subjected to the following conditions: 1 cycle of 2 min at 92°C, 34 cycles of 60 s at 92°C, 90 s at 60°C, and 110 s at 72°C, and 1 cycle of 7 min at 72°C, then held at 6°C. An 11 μl aliquot of each PCR mixture was electrophoresed through a 2% agarose gel. Samples yielding an appropriately sized amplified product (~190 bp) were considered positive for the transgene. Mice carrying a CK19-hPAP transgene [CK19-hPAP; TgN(Ck19ALPP)6Eps] were described previously (4). This transgene targets hPAP to CK19-expressing cells, including pancreatic ductal epithelial but not acinar cells. Treatment with 0.17 mg/ml BCIP (Sigma, St. Louis, MO) substrate overnight at 37°C yields a blue reaction product over the hPAP-expressing cells. Bitransgenic mice were generated by crossing two separate lines of mice. All of the mice were housed in Association for Assessment and Accreditation of Laboratory Animal Care-accredited facilities and used in accordance with the NIH Guide for the Care and Use of Laboratory Animals. The Ela-$Kras^{G12D}$ transgenic lineage 1366–5 has been assigned the following genetic designation: TgN(Ela1$KRAS^{G12D}$)9EPS.

Microscopic Analysis and Immunohistochemistry. Mice were administered 200 mg/kg body weight BrdUrd (Sigma) via i.p. injection, then euthanized 1–2 h later and examined for gross abnormalities. Tissues were fixed in Carnoy's fixative, paraffin-embedded, sectioned, mounted on a slide, and

Received 12/20/02; accepted 3/18/03.

The costs of publication of this article were defrayed in part by the payment of page charges. This article must therefore be hereby marked *advertisement* in accordance with 18 U.S.C. Section 1734 solely to indicate this fact.

[1] Supported by NIH Grants (RO1-CA76361) and American Cancer Society (DB-76; to E. P. S.), and funds from the Gieger Foundation (to P. J. G. and M. J. D).

[2] Present address: Department of Surgery, Northwestern University Feinberg School of Medicine, Chicago, IL 60611.

[3] Present address: Department of Surgery, University of Arizona Health Sciences Center, Tucson, AZ 85724.

[4] To whom requests for reprints should be addressed, at School of Veterinary Medicine, University of Wisconsin-Madison, 2015 Linden Drive, Madison, WI 53706. Phone: (608) 263-8870; Fax: (608) 265-8435; E-mail: sandgren@svm.vetmed.wisc.edu.

[5] The abbreviations used are: Ela, elastase; AB/PAS, alcian blue/periodic acid Schiff's; BrdUrd, bromodeoxyuridine; CK19, cytokeratin 19; hPAP, human placental alkaline phosphatase; BCIP, 5-bromo-4-chloro-3-indolyl phosphate; RT-PCR, reverse transcription-PCR; LCM, laser capture microdissection; NFR, nuclear fast red; CIS, carcinoma *in situ*.

stained with H&E or AB/PAS for microscopic examination. Unstained sections were used for labeling with antibodies or for hPAP staining. Immunohistochemistry followed standard procedures (4), with overnight exposure at room temperature to primary antibody diluted in 0.5% nonfat milk. The mouse monoclonal anti-Kras (Santa Cruz Biotech, Santa Cruz, CA) was diluted 1:20. The rat monoclonal anti-BrdUrd (Accurate Scientific, Westbury, NY) was diluted 1:40. The rat monoclonal anti-CK19 (TROMA 3; a gift of Dr. Rolf Kemler, Max Planck Institute, Freiburg, Germany) was diluted 1:100. Irrelevant primary antibodies of the same species were used as controls. Sections next were incubated sequentially with species-specific link antibody (BioGenex, San Ramon, CA), peroxidase enzyme label (BioGenex), and diaminobenzidine (Sigma), then stained with hematoxylin (Polysciences, Inc., Warrington, PA) or nuclear fast red (PolyScientific, Bay Shore, NY), dehydrated, and mounted under a glass coverslip.

RT-PCR/RFLP Analysis and Sequencing of PCR Product. Fresh or frozen tissue was homogenized in TRIzol (Invitrogen, Carlsbad, CA) at about 0.1 g/ml. RNA was isolated and cDNA prepared according to the manufacturer's instructions. cDNA from each sample was amplified via PCR using two specific primers: 5′-CATTGCACTGTACTCCTCTTGACCTG-3′ and 5′-ACTGAATATAAACTTGTGGTAGTTGGACCT-3′. The 5′ primer included a single nucleotide substitution that introduced a *Bst*NI restriction endonuclease site and contained sequences that included codon 12. The 3′ primer was designed to complement sequences in the second exon to distinguish amplified genomic DNA and cDNA. The PCR conditions were as follows: 95°C for 5 min, 35–45 cycles of 95°C for 30 s, 54°C for 1 min, and 72°C for 45 s, and a 5 min cycle at 72°C. PCR product was incubated with *Bst*NI restriction enzyme. Fragments were analyzed on 6% polyacrylamide gels stained with ethidium bromide. For some samples, product was sequenced using an ABI 310 sequencer. Primers for β-actin (5′-GGCATCGTGATGGACTCCG-3′ and 5′-GCTGGAAGGTGGACAGCGA-3′) were used to evaluate the relative quantity of RNA from most samples.

LCM RT-PCR/RFLP Analysis. Pancreatic tissues from Ela-Kras mice were fixed, cut into 5–10 μm sections, and mounted on plain glass slides. The slides were stained with H&E and dehydrated in graded alcohols and xylene. LCM was performed on the stained sections using a PixCell II laser capture microscope (Arcturus Engineering Inc., Mountain View, CA). RNA was isolated by incubating the tissue section in 10 μl guanidine isothiocyanate buffer [5.25 M guanidinium isothiocyanate, 50 mM Tris-Cl (pH 6.4), 20 mM EDTA, 1% Triton X-100, and 0.1 M β-mercaptoethanol] on the cap, fitting a microfuge tube over the cap, and incubating at 42°C for 30–60 min. RNA was extracted with chloroform and precipitated twice. cDNA was prepared and amplified via PCR as described above.

Results and Discussion

We identified 10 founder mice that carried the Ela-Kras^{G12D} transgene encoding the Kras codon 12 aspartate mutant. Eight were smaller than normal at birth and had distended abdomens. On gross examination, pancreases from this group of mice were white, firm, and nodular or polycystic. Microscopically, there were occasional normal-appearing acini, but most pancreatic tissue was abnormal (Fig. 1, *A–C*), containing an often-extensive stroma adjacent to dysplastic epithelium with a glandular or papillary organization (Fig. 1*B*), and lacking normal ducts. In one founder, the pancreas was composed of ductal structures lined by epithelial cells that were intensely positive for the histochemical stain AB/PAS (Fig. 1*C*), consistent with the presence of mucins, complex glycoproteins that are produced normally only by epithelial cells in larger pancreatic ducts. A similar phenotype accompanied expression of mutant Hras in this tissue (19). Thus, presence in fetal exocrine pancreas of a constitutively activated ras protein can induce diffuse hyperplasia and interfere with normal epithelial differentiation. These findings indicate that fetal pancreas cells possess intact and functional ras-responsive cell signaling pathways, implying that H- and/or K-ras may have a role in normal pancreatic development.

Two of the 10 founder mice appeared normal at birth, and these were mated to produce lineages. In the best-characterized line, 1366–5, all of the males but no females carried the transgene, indicating transgene integration into the Y chromosome. Perinatal transgenic mice in either line had normal-appearing pancreases that contained occasional hyperplastic acini (Fig. 1*D*). Survival of these founder mice was likely a consequence of reduced transgene expression in fetal pancreas, perhaps associated with the site of transgene integration. However, as mice in line 1366–5 aged, more extensive pancreatic lesions developed (Fig. 1*E*), including multifocal acinar hyperplasia and, less commonly, tubular complexes, consisting of acinar-like structures with a prominent central lumen (Fig. 1*E*). These lesions persisted throughout the life span of transgenic mice, although this phenotype was most severe in 1–2-month-old mice. Frequently, acinar lesions were accompanied by focal dysplasia, fibrosis, and/or lymphocytic infiltration. We observed no lesions involving ductal epithelium in young mice. Aging also was accompanied by exocrine pancreatic atrophy, and survival of transgenic mice was reduced, with occasional mice losing condition and requiring sacrifice beginning at 1 year of age.

A striking finding in older transgenic mice was the consistent development of acinar-to-ductal metaplasia. A few acinar lesions in mice 6–18 months of age displayed morphological changes suggesting acquisition of a ductular phenotype. These transitional structures were composed of heterogeneous cells that ranged from acinar-like (with basal nucleus and zymogen granules) to duct-like (smaller, with a central nucleus; Fig. 1*F*), and that occasionally displayed dark purple staining in apical cytoplasm when treated with AB/PAS (Fig. 1*F*). Acinar to ductal metaplasia also was suggested by analysis of hsEla-Kras^{G12D}/CK19-hPAP bitransgenic mice. CK19-hPAP is expressed in simple epithelium, including pancreatic ductal epithelium, but not in acinar cells (Fig. 1*G*; Ref. 4). Pancreases from bitransgenic mice displayed multifocal areas of abnormal hPAP staining relative to mice carrying only the CK19-hPAP (Fig. 1*H*). Hyperplastic acini and tubular complexes, together with some adjacent normal-appearing acini, exhibited variably intense hPAP staining. This finding indicated activation of CK19 expression in these cells despite their apparent acinar cell origin and morphology. Epithelial structures with distinct lumens and reduced acinar cell differentiation displayed the highest level of staining (Fig. 1, *I* and *J*).

BrdUrd labeling index (representing the fraction of cells undergoing DNA synthesis) was increased slightly in morphologically normal acinar cells of Ela-Kras^{G12D} transgenic mice compared to nontransgenic control mice (Table 1). Labeling index was increased even more in both hyperplastic acini and tubular complexes.

Beginning at 11 months of age, 18 of 40 line 1366–5 transgenic mice that were examined developed lesions with microscopic features of neoplasia. Three of these 40 transgenic mice developed noninvasive acinar cell hyperplasias/adenomas. Cells in these lesions resembled acinar cells, but they displayed increased eosinophilia, increased nuclear:cytoplasmic ratio, and loss of typical acinar architecture (data not shown). Fourteen of 40 Ela-Kras^{G12D} mice displayed one to several variably sized cystic structures lined by a single layer of epithelial-like cells that often formed papillary projections into a central lumen (Fig. 1, *K–M*). Epithelial cells in many of these lesions stained dark purple with AB/PAS (Fig. 1*L*). One ductular structure that developed in an Ela-Kras^{G12D}/CK19-hPAP 11-month-old bitransgenic mouse also stained intensely for hPAP, confirming the expression of CK19. Cells in these duct-like lesions also demonstrated increased BrdUrd labeling index (Table 1) and the presence of CK19 protein (Fig. 1*M*). The elevated rate of DNA synthesis and the presence of severe cellular dysplasia indicate that some of these lesions had progressed to a stage of CIS. Several lesions resembled intraductal papillary mucinous carcinomas identified in some human patients. Importantly, ductal lesions did not progress beyond the

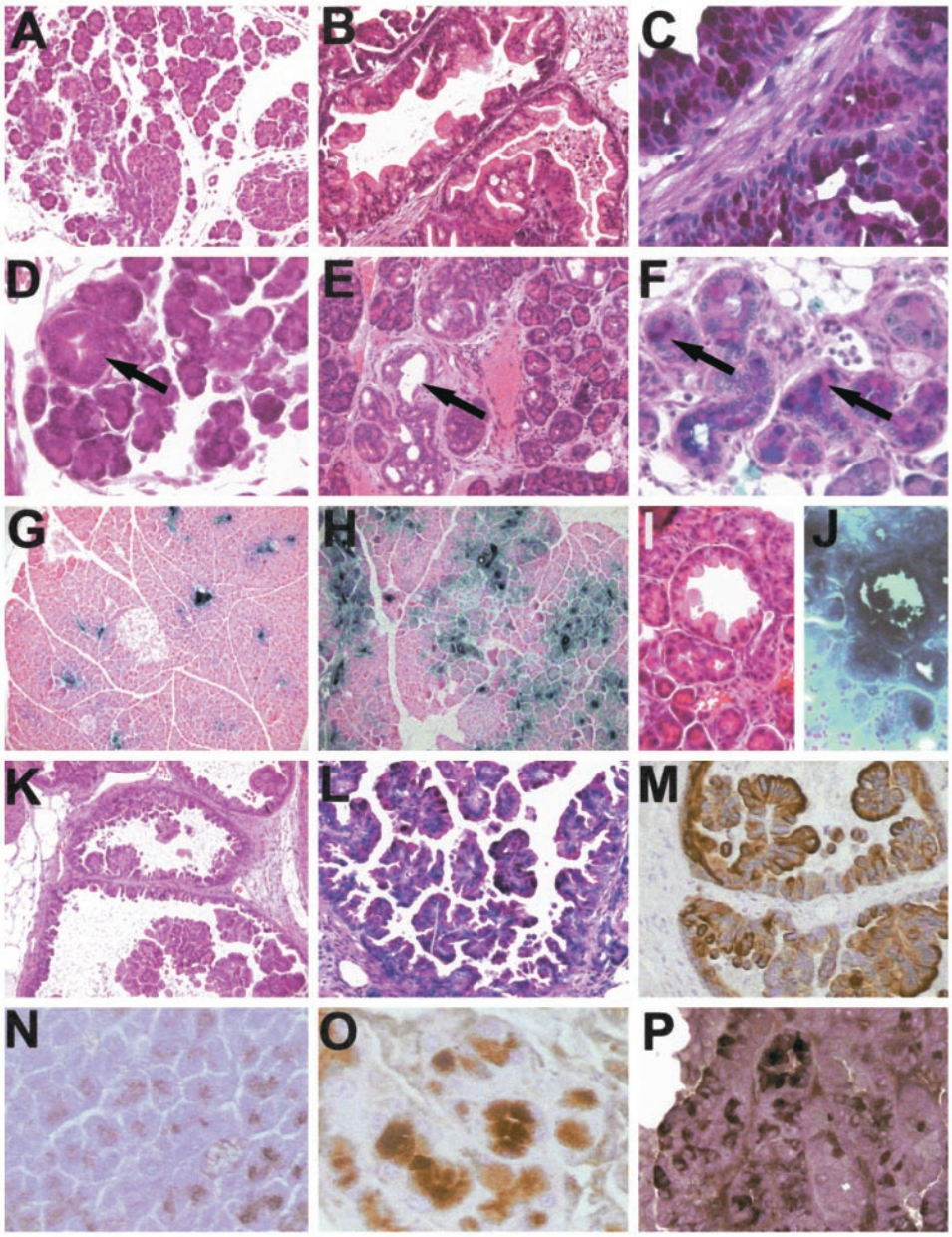

Fig. 1. hsEla-Kras^{G12D} transgenic mouse pancreatic lesions. *A,* nontransgenic neonatal mouse pancreas; H&E. *B,* transgenic founder neonatal mouse pancreas; H&E. Note the projections of papillary epithelium into the lumens of large duct-like structures. *C,* same as *B*; AB/PAS. *Dark purple-stained* papillary epithelial cells suggest the presence of the duct cell marker mucin. *D,* line 1366–5 transgenic neonatal mouse pancreas; H&E. Note one hyperplastic acinus (*arrow*), but most acini appear normal. *E,* line 1366–5 transgenic adult mouse pancreas; H&E. Note increased interacinar stroma and multiple tubular complexes with large centroacinar spaces lined by flattened acinar cells (*arrow*). *F,* line 1366–5 transgenic adult mouse pancreas; AB/PAS. Note several transitional structures composed of cells with acinar morphology and other cells that stain *dark purple* (*arrows*), suggesting presence of the duct cell marker mucin. *G,* CK19-hPAP transgenic adult mouse pancreas; BCIP/NFR stain. *Blue stain* indicates hPAP enzymatic activity. In normal pancreas, CK19 expression is restricted to ductal epithelial cells, with some background staining over RBCs in large vessels. *H,* CK19-hPAP/hsEla-Kras^{G12D} line 1366–5 bitransgenic young adult mouse pancreas; BCIP/NFR stain. Ducts remain stained, but many acini also display stain, indicating activation of CK19 transgene expression. *I,* CK19-hPAP/hsEla-Kras^{G12D} line 1366–5 bitransgenic young adult mouse pancreas; H&E. Note the small ductal structure with prominent lumen. *J,* adjacent section to *K*; BCIP/NFR stain. The ductal cells and adjacent acinar cells express the CK19-hPAP transgene. *K,* line 1366–5 transgenic 16-month-old mouse pancreas; H&E. In the *center* of the panel is a lesion resembling a noninvasive intraductal papillary-mucinous carcinoma. *L,* as in *M*; AB/PAS. Papillary epithelial cells often contain apical mucin (*dark purple*). *M,* line 1366–5 transgenic 16-month-old mouse pancreas; immunohistochemistry to detect mouse CK19 protein. Epithelial cells in the duct-like lesion contain this duct cell marker protein, which is not present in normal acinar cells. *N,* nontransgenic adult mouse pancreas; immunohistochemistry to detect Kras protein. Faint staining is present in acinar cells (staining is not present when using an irrelevant primary antibody; data not shown). *O,* line 1366–5 transgenic adult mouse pancreas; immunohistochemistry to detect Kras protein. Staining in acinar cells is variable, but focally intense. *P,* line 1366–5 transgenic 21-month-old mouse pancreas; immunohistochemistry to detect Kras protein. Note strong staining in some cells in this papillary CIS lesion and no staining in others. Original magnifications: *G and H,* ×40; *A–C, E,* and *K,* ×100; *D, F, I, J, L,* and *M,* ×200; *N–P,* ×400.

preinvasive stage. We also examined pancreas morphology in a second line (1643–5) of Ela-Kras^{G12D} transgenic mice derived from a surviving founder mouse. Although pancreatic lesions were less frequent in this line, 4 mice over 16 months of age developed lesions composed of cells with ductal phenotype resembling those observed in line 1366–5, and 1 mouse developed a 1.5-cm diameter acinar cell carcinoma. Thus, lesion development was not restricted to a single lineage.

Table 1 *BrdUrd labeling indices in pancreatic lesions of Ela-Kras^{G12D} line 1366-5 transgenic mice*

	Lesion type			
Mice	Normal acinar morphology	Acinar hyperplasia	Tubular complex	Ductal[a]
Nontransgenic	0.25 ± 0.33 (4)[b]	-	-	-
Transgenic	1.0 ± 0.9 (11)	9.0 ± 5.8 (11)	5.8 ± 4.1 (18)	7.4 ± 3.0 (14)

[a] Ductal indicates uniform ductal morphology and expression of CK19.
[b] Data presented as % BrdU-labeled nuclei ± SD (no. analyzed).

To evaluate transgene expression, we identified Kras protein using immunohistochemistry, and mRNA using RT-PCR and subsequent DNA sequencing. The antibody was not specific for mutant Kras, and acinar cells in nontransgenic mice displayed faint cytoplasmic immunoreactivity (Fig. 1*N*). In transgenic mice, most acinar cells displayed strong immunoreactivity, indicating an increase in Kras protein, although cells in the same lobules displayed staining similar to that in nontransgenic mouse pancreas (Fig. 1*O*). Cells present in acinar lesions also displayed strong anti-Kras immunoreactivity. The presence of transgene product was confirmed by RT-PCR/RFLP analysis, which demonstrated both wild-type (endogenous) and mutant Kras transcripts in transgenic mouse pancreas (Fig. 2, *left*). When sequenced, transcripts displayed the expected G to A transition in codon 12 (data not shown). We also examined transgene expression in the preinvasive ductal lesions. Most ductal lesions contained immunohistochemically detectable Kras (Fig. 1*P*), although only a subset of cells in each lesion was Kras positive (5–80% positive; mean 40%). RT-PCR/RFLP analysis performed on ductal lesion epithelium col-

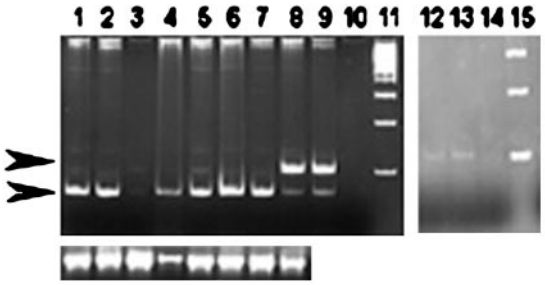

Fig. 2. RT-PCR/RFLP evaluation of pancreatic Kras expression. *Bottom band* (*bottom arrowhead*) represents endogenous Kras amplified message. *Top band* (*top arrowhead*) represents transgene-specific mutant Kras amplified message. *Left panel,* analysis of whole tissue. *Lanes 1–4*, nontransgenic mouse tissues; *Lanes 5–9*, hsEla-Kras^{G12D} line 1366–5 transgenic mouse tissues. *Lanes 1* and *5*, liver; *Lanes 2* and *6*, kidney; *Lanes 3* and *7,* spleen; *Lanes 4, 8,* and *9*, pancreas; *Lane 10,* water; *Lane 11,* molecular weight standard. Note the presence of transgene Kras RNA only in pancreas, and endogenous Kras RNA in all tissues. *Panels below Lanes 1–8* display bands amplified by β-actin primers. *Right panel,* analysis of LCM-generated tissue samples. *Lane 12*, duct-like CIS lesion RNA; *Lane 13*, transgenic mouse acinar cells; *Lane 14,* water; *Lane 15,* molecular weight standard. Mutant Kras-specific product is visible in the ductal lesion and acinar cells collected from the transgenic mouse pancreas.

lected via LCM demonstrated the presence of transgene Kras transcript (Fig. 2, *right*), indicating that transgene expression is not extinguished during lesion development. This finding, in turn, indicates that failure of lesions to progress to an invasive stage was not the result of loss of transgene expression.

Our findings demonstrate that Kras^{G12D} can initiate development of preinvasive ductal neoplasia in exocrine pancreas of adult mice. Because of the focal nature of these lesions and their appearance in older mice, other cellular alterations also must be involved. Most striking, these ductal lesions appear to arise from acinar cells. The development of ductal lesions from acinar cells may seem counterintuitive. However, many studies have suggested that human, mouse, rat, guinea pig, and hamster acinar cells can redifferentiate into cells with ductal characteristics after isolation and culturing *in vitro* (5–12). In transgenic mice expressing transforming growth factor α in acinar cells, tubular complexes developed that contained cells expressing ductal markers (13–16). Ela-c-myc transgenic mice developed both acinar cell carcinomas and mixed acinar/ductal carcinomas, most likely as a result of metaplasia (17). These mixed neoplasms contained CK19 and AB/PAS-positive cells embedded within a dense stroma. However, unlike ductal lesions in hsEla-Kras^{G12D} transgenic mice, Ela-c-myc neoplasms always contained a morphologically identifiable neoplastic acinar cell component (17). Our data indicate that targeting of Kras^{G12D} to acinar cells also can initiate this metaplastic transition. These studies do not rule out the possibility that a nonacinar cell, such as an islet cell or multipotent stem cell present in adult pancreas, can serve as a progenitor for some ductal lesions. However, the finding of tubular complexes lined by both acinar and ductal cells suggests that acinar- or centroacinar-to-ductal metaplasia accounts for at least some of the ductal lesions observed. Unfortunately, it has not been possible to target transgenes specifically to pancreatic ductal epithelium. Thus, there remains an important need to express mutant Kras in pancreatic ductal epithelium to compare both the morphology and progression of resulting lesions with those described above.

We have established a mouse model of mutant Kras-induced preinvasive pancreatic neoplasia with lesions composed entirely of cells with ductal phenotype. This model reproduces both the most commonly identified genetic alteration and the most frequent cellular histotype diagnosed in the human disease. In this model, Kras^{G12D} is not sufficient to induce progression to the invasive stage of carcinoma; lesions appear to be arrested at the preinvasive stage despite confirmed Kras expression in at least some lesion epithelial cells. Consistent with this finding, *Kras* mutation has been proposed to be an early step in the development of human pancreatic adenocarcinoma (3, 20). Arrest at an early stage of tumor progression is a strength of the Ela-Kras^{G12D} model; these mice will allow us to alter selectively the status of other genes implicated in the human disease and systematically define their ability to complement mutant Kras during pancreatic carcinogenesis in an intact animal.

Acknowledgments

We thank Dr. Richard Palmiter and Dr. Manuel Perucho for providing DNA clones; and Cathleen Berglund, Ryan Cassaday, Kara Doffek, Paul Schaus, Renee Szakaly, and Kari Witte for technical assistance.

References

1. Greenlee, R. T., Hill-Harmon, M. B., Murray, T., and Thun, M. Cancer statistics, 2001. CA Cancer J. Clin., *51:* 15–36, 2001.
2. Almoguera, C. Shibata, D., Forrester, K., Martin, J., Arnheim, N., and Perucho, M. Most human carcinomas of the exocrine pancreas contain mutant c-K-ras genes. Cell, *53:* 549–554, 1988.
3. Hilgers, W., and Kern, S. E., Molecular genetic basis of pancreatic adenocarcinoma. Genes Chromosomes Cancer, *26:* 1–12, 1999.
4. Grippo, P. J., and Sandgren, E. P. Highly invasive transitional cell carcinoma of the bladder in a simian virus 40 T-antigen transgenic mouse model. Am. J. Pathol., *157:* 805–813, 2000.
5. De Lisle, R. C., and Logsdon, C. D. Pancreatic acinar cells in culture: expression of acinar and ductal antigens in a growth-related manner. Eur. J. Cell Biol., *51:* 64–75, 1990.
6. Scarpelli, D. G., Rao, M. S., and Reddy, J. K. Are acinar cells involved in the pathogenesis of ductal adenocarcinoma of the pancreas? Cancer Cells (Cold Spring Harbor), *3:* 275–277, 1991.
7. Hall, P. A., and Lemoine, N. R. Rapid acinar to ductal transdifferentiation in cultured human exocrine pancreas. J. Pathol., *166:* 97–103, 1992.
8. Arias, A. E., and Bendayan, M. Differentiation of pancreatic acinar cells into duct-like cells *in vitro*. Lab. Investig., *69:* 518–530, 1993.
9. Pettengill, O. S., Faris, R. A., Bell, R. H., Jr. Kuhlmann, E. T., Longnecker, D. S. Derivation of duct-like cell lines from a transplantable acinar cell carcinoma of the rat pancreas. Am. J. Pathol., *143:* 292–303, 1993.
10. Vila, M. R., Lloreta, J., and Real, F. X. Normal human pancreas cultures display functional ductal characteristics. Lab. Investig., *71:* 423–431, 1994.
11. Yuan, S., Duguid, W. P., Agapitos, D., Wyllie, B., and Rosenberg, L. Phenotypic modulation of hamster acinar cells by culture in collagen matrix. Exp. Cell Res., *237:* 247–258, 1997.
12. Flaks, B., Moore, M. A., and Flaks, A. Ultrastructural analysis of pancreatic carcinogenesis. V. Changes in differentiation of acinar cells during chronic treatment with N-nitrosobis(2-hydroxypropyl)amine. Carcinogenesis (Lond.), *3:* 485–498, 1982.
13. Sandgren, E. P., Luetteke, N. C., Palmiter, R. D., Brinster, R. L., and Lee, D. C. Overexpression of transforming growth factor α in transgenic mice: induction of epithelial hyperplasia, pancreatic metaplasia, and carcinoma of the breast. Cell, *61:* 1121–1135, 1990.
14. Bockman, D. E., and Merlino, G. Cytological changes in the pancreas of transgenic mice overexpressing transforming growth factor α. Gastroenterology, *103:* 1883–1892, 1992.
15. Wagner, M., Luhrs, H., Kloppel, G., Adler, G., and Schmid, R. M. Malignant transformation of duct-like cells originating from acini in transforming growth factor α transgenic mice. Gastroenterology, *115:* 1254–1262, 1998.
16. Wagner, M. Greten, F. R., Weber, C. K., Koschnick, S., Mattfeldt, T., Deppert, W., Kern, H., Adler, G., and Schmid, R. M. A murine tumor progression model for pancreatic cancer recapitulating the genetic alterations of the human disease. Genes Dev., *15:* 286–293, 2001.
17. Sandgren, E. P., Quaife, C. J., Paulovich, A. G., Palmiter, R. D., and Brinster, R. L. Pancreatic tumor pathogenesis reflects the causative genetic lesion. Proc. Natl. Acad. Sci. USA, *88:* 93–97, 1991.
18. Palmiter, R. D., Sandgren, E. P., Koeller, D. M., and Brinster, R. L. Distal regulatory elements from the mouse metallothionein locus stimulate gene expression in transgenic mice. Mol. Cell. Biol., *13:* 5266–5275, 1993.
19. Quaife, C. J., Pinkert, C. A., Ornitz, D. M., Palmiter, R. D., and Brinster, R. L. Pancreatic neoplasia induced by ras expression in acinar cells of transgenic mice. Cell, *48:* 1023–1034, 1987.
20. Hruban, R. H., Wilentz, R. E., and Kern, S. E. Genetic progression in the pancreatic ducts. Am. J. Pathol., *156:* 1821–1825, 2000.

Preinvasive Pancreatic Neoplasia of Ductal Phenotype Induced by Acinar Cell Targeting of Mutant Kras in Transgenic Mice

Paul J. Grippo, Patrick S. Nowlin, Michael J. Demeure, et al.

Cancer Res 2003;63:2016-2019.